

Chemical Science



Accepted Manuscript

This article can be cited before page numbers have been issued, to do this please use: F. Frateloreto, G. Capocasa, M. De Angelis, G. Sandri, O. Lanzalunga, C. Massera and S. Di Stefano, *Chem. Sci.*, 2025, DOI: 10.1039/D5SC07665J.



This is an Accepted Manuscript, which has been through the Royal Society of Chemistry peer review process and has been accepted for publication.

Accepted Manuscripts are published online shortly after acceptance, before technical editing, formatting and proof reading. Using this free service, authors can make their results available to the community, in citable form, before we publish the edited article. We will replace this Accepted Manuscript with the edited and formatted Advance Article as soon as it is available.

You can find more information about Accepted Manuscripts in the <u>Information for Authors</u>.

Please note that technical editing may introduce minor changes to the text and/or graphics, which may alter content. The journal's standard <u>Terms & Conditions</u> and the <u>Ethical guidelines</u> still apply. In no event shall the Royal Society of Chemistry be held responsible for any errors or omissions in this Accepted Manuscript or any consequences arising from the use of any information it contains.



Received 00th January 20xx, Accepted 00th January 20xx View Article Online DOI: 10.1039/D5SC07665J

ARTICLE

The Dynamic Chemistry of the Boron-Nitrogen Bond

Federico Frateloreto,*,a,§ Giorgio Capocasa,*a,§ Martina De Angelis,a,§ Greta Sandri,a Osvaldo Lanzalunga,a Chiara Massera*,b and Stefano Di Stefano*,a

Here we report that fully reversible $B \leftarrow N$ bond formation/cleavage is a promising tool for the achievement of dynamic libraries (DLs) of rapidly interconverting compounds. The composition of a number of minimal DLs of adducts between phenylboronic acid catechol ester 1 and a series of nitrogen-based aromatic heterocycles (NArHets) is demonstrated to be predictable taking into account the association constants related to the formation processes of the single adducts involved. Furthermore, such composition can be controlled over time by the use of activated carboxylic acids (ACAs). Depending on the amount of added ACA, a $B \leftarrow N$ based DL can be either overturned in terms of composition, transiently overexpressing an adduct initially underexpressed, or transiently fully disassembled into its building blocks.

Introduction

DOI: 10.1039/x0xx00000x

This article is licensed under a Creative Commons Attribution 3.0 Unported Licence.

oen Access Article. Published on 27 November 2025. Downloaded on 28.11.2025 04:14:48.

Dynamic combinatorial chemistry (DCC)1-8 has been an intense field of investigation since two decades due to its implications in different topics such as supramolecular recognition,9-12 catalysis, 13-17 dissipative, 18-29 and systems chemistry. 30-36 Both covalent and supramolecular reversible bonds have been largely employed to constitute dynamic libraries (with this term, DLs, one typically refers to collections of compounds able to interconvert by exchanging building blocks under equilibrium conditions), with the latter generally having the advantage of very fast kinetics on human scale. Nevertheless, the presence of a catalyst may confer the same feature also to covalent dynamic bonds such as imine, acetal, olefin bonds and the like. Here we report on a systematic investigation of the exchange reactions involving the Lewis-pairs formed by phenylboronic acid catechol ester (1) and several nitrogen-based aromatic heterocycles, NArHets -namely a series of pyridines and N-methylimidazole. Such reaction entails the formation/cleavage of the dynamic, covalent (dative) B←N bond. The process turns out to be fast on the human timescale and fully reversible, even in the absence of any catalyst. The B←N exchange process involving catechol boronic esters and NArHets has been already exploited to build a variety of complex molecular structures. 37-40 Several examples involve the achievement of macrocycles,41-45 molecular cages, 46,47 rotaxanes, 48,49 supramolecular adducts, $^{50\cdot55}$ covalent organic frameworks (COFs), $^{56\cdot61}$ and polymeric materials. $^{62\cdot67}$ However, despite the episodic use of the B \leftarrow N bond in the design of (supra)molecular architectures, we feel that a systematic investigation of its properties is still missing. In this work, we aim to build a deeper mechanistic comprehension of the properties of such bond and to frame the B \leftarrow N Lewis pair formation within the field of dynamic combinatorial chemistry as a versatile tool for the generation of DLs.

Experimental section

Materials

All the NArHets, amines, catechol, phenylboronic acid, and tribromoacetic acid were purchased from Fluorochem, TCI or Merck. Deuterated chloroform was purchased from Fluorochem. Non-deuterated solvents were purchased from Carlo Erba. Deuterated chloroform was passed through short plugs of Na₂SO₄ (anhydrous) and Al₂O₃ (activated, basic) before use to remove excess water and traces of acids. NMR spectra were recorded on either a BrukerDPX300 or a BrukerDPX400 spectrometer and were internally referenced to the residual proton solvent signal. See ESI for further details.

^a Dipartimento di Chimica, Università di Roma La Sapienza and ISB-CNR Sede Secondaria di Roma - Meccanismi di Reazione, P.Ie A. Moro 5, I-00185 Roma, Italy, E-mail: federico.frateloreto@uniroma1.it, giorgio.capocasa@uniroma1.it, stefano.distefano@uniroma1.it.

^b Dipartimento di Scienze Chimiche, della Vita e della Sostenibilità Ambientale, Università degli Studi di Parma, Parco Area delle Scienze 17/A, 43124 Parma, Italy, E-mail: chiara.massera@unipr.it.

[§] These authors contributed equally.

[†] Electronic Supplementary Information (ESI) available: details on the synthesis of **1**, titration of **1** with NArHets **2-6**, crystallographic data, NMR spectra, ORCA input and output files, and speciation of the DDLs obtained. See DOI: 10.1039/x0xx00000x

ARTICLE Journal Name

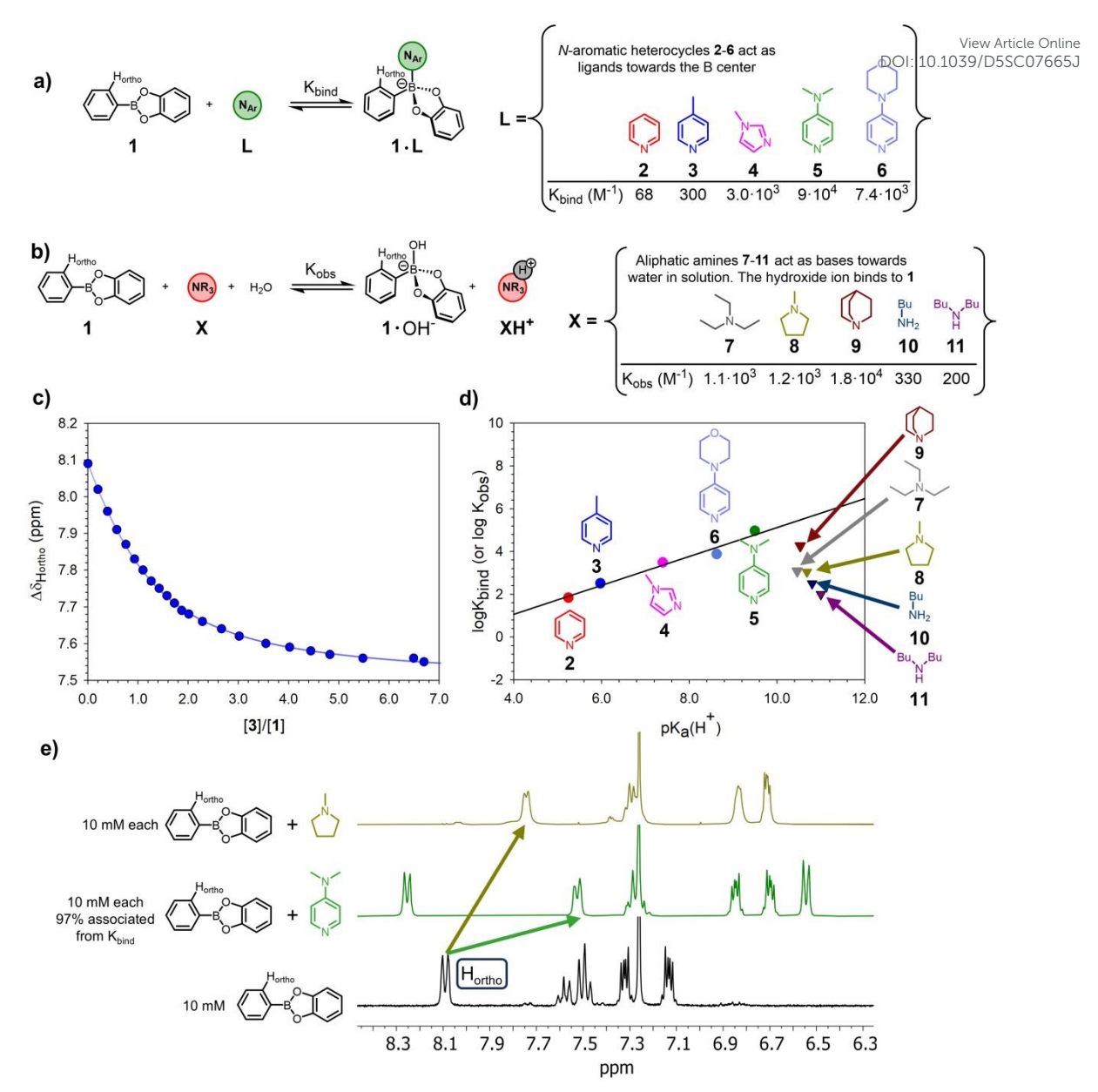


Fig. 1 a) Binding processes between phenylboronic acid catechol ester 1 and NArHets 2-6. b) Overall proposed transformation occurring in the presence of amines 7-11. c) ¹H-NMR titration of 5.0 mM 1 with 3 in CDCl₃ at 25 °C (see ESI, Figures S23-S32 for the other titrations). d) Brønsted correlation between log K_{blind} (or log K_{obs}, for aliphatic amines 7-11) and pK_aH⁺ for compounds 2-11 (for pyridines, ρ = 0.68, R² = 0.97, see ESI, Table S2 for details). The linear correlation only holds for NArHets 2-6; the data points relative to amines 7-11 lay outside the line. e) Comparison of ¹H-NMR traces of 1 (bottom, black), a mixture of 1 and 5 (centre, green), and a mixture of 1 and 8 (top, gold). Spectra recorded at 25 °C; all compounds are 10 mM in CDCl₃. Only the aromatics portion is shown. See Figures S51 for full spectra. The H_{ortho} protons on the phenyl moiety on 1 are rendered equivalent in the ¹H-NMR spectra by the fast rotation about the Ph–B bond.

Synthesis of 1

Catechol (451 mg, 4.1 mmol) was added to a dichloromethane (14 mL) suspension of phenylboronic acid (500 mg, 4.1 mmol). Then, ethyl acetate was added dropwise under stirring until a homogeneous solution was obtained. The resulting mixture was stirred at room temperature overnight. The solution was dried over anhydrous Na_2SO_4 , filtered, and concentrated under reduced pressure. Recrystallization from hot hexane afforded 1 as clear needle-like crystals (650 mg, 81%). See ESI for further information.

Results and discussion

Firstly, a series of titration experiments was carried out in order to quantify the strength of the interaction between phenylboronic acid catechol ester **1**, which can be considered a benchmark boron-based substrate, and a series of NArHets in CDCl₃ at 25 °C, see Figure 1a for the relevant equilibria.

The equilibrium constants (K_{bind}) for the formation of complexes $\mathbf{1} \cdot \mathbf{L}$ with $\mathbf{L} = \{\mathbf{2} \cdot \mathbf{6}\}$ were obtained by plotting the chemical shift of the 1H NMR signal of proton H_{ortho} on $\mathbf{1}$ against the NArHets concentration. A 1:1 binding model was fitted to the experimental data. (see Figure 1c for the case of the $\mathbf{1} \cdot \mathbf{3}$ adduct and ESI for the other cases). For complexes $\mathbf{1} \cdot \mathbf{2}$ and $\mathbf{1} \cdot \mathbf{5}$, the

Journal Name ARTICLE

obtained K_{bind} are in good accordance with the values previously measured in the same solvent. $^{38}\,$

Upon addition of NArHets 2-6 to a solution of 1, the formation of complexes 1 • (2-6) occurs immediately and smoothly with no detectable side-product accumulating in solution. These equilibria are fast on the ¹H NMR timescale, as evidenced by the resolved signals (Figure 1e, green trace). Furthermore, the higher the pK_aH^+ of the employed heterocycle, the larger the K_{bind} with a very good log K_{bind} - $pK_aH^{\scriptscriptstyle +}$ Brønsted correlation (Figure 1d, $\rho = 0.68$, $R^2 = 0.97$. For any base, pK_aH^+ is the pK_a of its conjugate acid.[‡] All the pK_aH⁺ values are measured in water, see Table S2 and the related caption for details, as well as Figures S13-S22 for the titration curves and the NMR spectra). The addition of aliphatic amines 7-11 to a CDCl₃ solution of 1, also produced a shielding of the Hortho proton on 1 with concomitant deshielding of the protons on the amine backbone. Again, a 1:1 binding model could be fit to the experimental data. However, even though aliphatic amines 7-11 are more basic than NArHets 2-6, the obtained Kobs values were significantly lower than the K_{bind} values of most NArHets, with no clear dependence on the strength of the base (see Figure 1c).

Furthermore, in all cases, the ¹H NMR spectra feature broad signals and spurious peaks not belonging to any readily identifiable species (see Figure 1e, gold trace).

Additionally, while the saturation value for the Hortho chemical shift was the same in all the titrations of 1 with NArHets 2-6 (namely 7.50 ppm, with 4 leading to the only slight outlier of 7.57 ppm), no clear pattern was found for aliphatic amines. (All the titration curves are reported in the SI. See Figures S23-S32) Taken together, this evidence points towards different reactivities of 1 in the presence of NArHets or aliphatic amines. Eventually, crystals were obtained from the 1:1 mixtures of 1 and amines 8 or 9. The structures feature the binding of a hydroxide ion to the B centre of 1 and the protonated amine engaging in H-bonding with the oxygen of the hydroxide group together with a water molecule (see Figure 2 and Tables S23 and S25). Although these are solid-state structures, we propose that the increased steric bulk around the nitrogen atom and higher basicity of aliphatic amines compared to NArHets favours the deprotonation of adventitious water in the chloroform and the subsequent coordination of the hydroxide ion to the boron (compare Figure 1a and Figure 1b), consistently with a reactivity model proposed by Anslyn.⁶⁸ This view is further supported by the fact that sterically bulky lutidine does not appreciably bind to 1 despite its increased basicity with respect to 3 (see Figure S34 and caption). Similarly, bulky phenylboronic acid pinacol ester is hardly reactive towards 5, the strongest binder for 1 employed in this work (Figure S36).

Since the formation of $\mathbf{1} \bullet \mathbf{HO}^-$ will occur to some extent every time that wet chloroform is employed, we tested whether its presence in large quantities would impact the formation of a B \leftarrow N complex. Therefore, to a 1:1 mixture of 1 and 7 (both 12.5 mM), an equimolar amount of 5 was added. The $^1\mathbf{H}$ NMR spectrum of the resulting mixture was very similar to that of the 1:1 mixture of 1 and 5, suggesting that, when possible, the formation of a B \leftarrow N complex is favoured with respect to that of

1•OH. A similar result, albeit less marked, was veltained by adding **4** in place of **5** (see Figures S51 and \$52).1039/D5SC07665J Having shown that the presence of **1•**OH is not detrimental to the formation of a B←N complex (or, more precisely, that **1•**OH and **1•L** with **L** = NArHet can co-exist as components of a DL, with **1•L** being the predominant species), we returned to characterising the B←N adducts.

All the adducts dissociate upon dilution and mass spectroscopy measurements are particularly difficult on the neutral compounds 1•L (L = 2-6) yielding no reliable information. Instead, for the definite identification of such adducts we resorted to X-ray crystallography which also provided us with valuable structural information. For compounds 1•2 and 1•5 it was possible to isolate single crystals suitable for X-ray analysis (Figure 2) by double layer crystallisation (chloroform/hexane) from 1 to 1 solution mixtures of the two components.

In the case of adduct 1.3, the crystals obtained were not suitable for diffraction analysis. However, the structure of this adduct has been previously solved and deposited in the Cambridge Structural Database (CSD)^{69,70} and has been used as reference in the present discussion. The crystallographic data and experimental details for data collection and structure refinement of 1.2 and 1.5 are reported in Table S23. The two adducts crystallise with more than one molecule in the asymmetric unit and their geometrical parameters are listed in Table S24. The B-N distances are all guite similar, ranging from 1.634(13) to 1.664(3) Å, with the exception of a slight outlier [1.607(7) Å] displayed by one of the three molecules in adduct 1.5. These values are in good agreement with the average distance of 1.645 Å obtained comparing 126 structures found in the CSD, all containing the B-N_{pyridine} fragment (see Tables S24 and S26).

Unfortunately, all the attempts to obtain single crystals of $1 \cdot 4$ and $1 \cdot 6$ failed. Nevertheless, on account of the similarities in the NMR spectra with the confirmed adducts, we propose that the prevalent process is that of $B \leftarrow N$ bond formation, rather than water deprotonation.

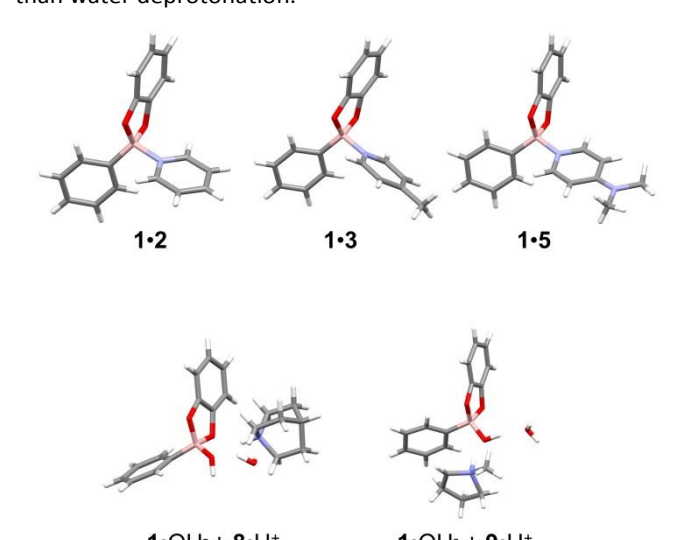


Fig. 2 X-ray structures. Top row: adducts 1•2, 1•3,70 and 1•5. Bottom row: co-crystals 1•0H' + 1•H' and 8•0H' + 9•H' Colour code: B, pink; N, blue; O, red; C, grey; H, white.

Journal Name

ARTICLE

In other to gain further insights into the nature of the B \leftarrow N bond occurring between **1** and the NArHets, a computational study was conducted. Calculations were performed with the ORCA 6.1.0 program package. The starting geometries of **1**, NArHets, and those of their adducts with **1** were optimised at the r²SCAN-3c level of theory, using the SMD solvation model (chloroform). Single point energies and frequences of the optimized structure were then computed at the r²SCAN-3c/def2-QZVPP(SMD) level of theory, following a benchmark study focused on Lewis acid-base interaction.

The stabilisation energies (Estab) of the interaction between 1 and NArHets were calculated as the difference between the energy of the adduct (Eadduct) and the sum of the energies of the donor NArHet (E_d), and the acceptor 1 (E_a), i.e. $E_{stab} = E_{adduct} - (E_d)$ + E_a).⁷⁶ E_{stab} values were then compared with those derivable from the experimentally measured binding constants. Figure 3 shows a good linear correlation between experimental and theoretical data, with a systematic discrepancy, on average, of about 0.57 kcal mol⁻¹(see Table S27). Moreover, the calculated B-N distances are comparable with those obtained from X-ray crystallography (see Table S28). To rationalise the similar Hortho chemical shift saturation values observed for the 1-NArHets adducts, Hirshfeld partial charges were computed (see Table S28). The averaged Hortho partial charges for each 1-NArHets range from 0.0313 for 1.5, to 0.0329 for 1.2 with the average value between all the adducts being 0.0321. These values are all very similar, but they are markedly different than the one obtained for free 1, which is 0.0479. The computed partial charges fit well with lower, very similar values of the Hortho chemical shift for all the adducts with respect to 1.

This article is licensed under a Creative Commons Attribution 3.0 Unported Licence.

oen Access Article. Published on 27 November 2025. Downloaded on 28.11.2025 04:14:48.

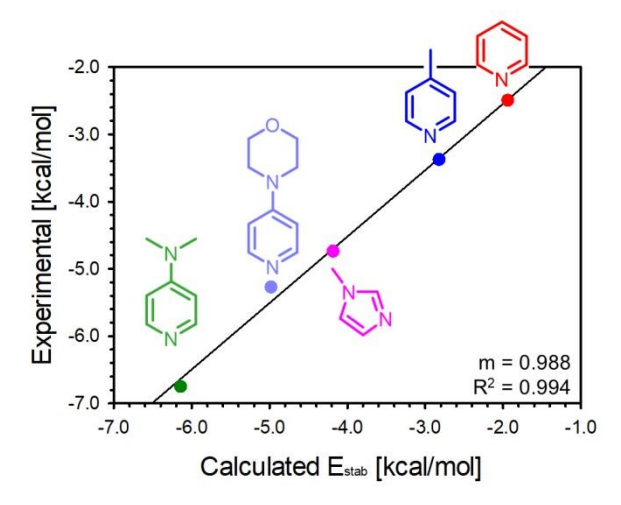


Fig. 3 Linear correlation between the experimental stabilization energies derived from K_{bind} measurements, and the computed stabilization energies for the 1-NArHet adducts.

Having gained some chemical understanding of the dynamic B←N bond, we turned to building and controlling dynamic libraries of increasing complexity by exploiting its properties. Therefore, six competitive experiments, each one involving two couples of adducts 1•L (with L = NArHets 2-5) were carried out in CDCl₃ at 25 °C as depicted in Figure 4, where the equilibrium for the couples 1•2 and 1•3 is shown. In all cases, compound 1

and the two given NArHets were added in equimolar amount (12.5 mM), and it was found that the exchange Peace of Was fast on ¹H NMR time scale, with the equilibrium reached immediately after the addition of the reagents (first spectrum recorded). Keq for each exchange reaction can be calculated from the ratio between the corresponding K_{bind} for each adduct. corresponds trace С which to in **Figure** $K_{eq} = K_{bind}(1 \cdot 3)/K_{bind}(1 \cdot 2) = 4.4$ with adduct $1 \cdot 3$ abundantly prevailing over 1•2 (free 1 30% of 1tot, 1•3 50% of 1tot and 1•2 20% of 1tot, see Figure S45 and the related caption in the ESI for details on the mixture composition obtained both experimentally and theoretically). As expected, since in the case of both adducts 1.2 and 1.3 the adopted conditions do not allow for a complete binding, the presence of two molar equivalents of bases (2 + 3 with respect to 1) in the competitive experiment causes a further up-field shift of all signals related to the boronic ester (identified by a black circle in Figure 4). As for the remaining five DLs the speciation was calculated and the theoretical amount of free 1 was satisfactorily compared to that calculated from NMR data (see ESI, Tables S7-S9). Being 4dimethylaminopyridine 5 the strongest binder versus ester 1, each time it is involved, the equilibrium is shifted toward adduct 1.5 (see Figures S47, S49, and S50). These experiments clearly demonstrate the ease of achieving DLs of B←N adducts able to rapidly interconvert on human timescale, with a predictable composition.

Next, we performed consecutive competition experiments, building DLs with an increased number of components (Figure 5 shows the reaction scheme, the NMR spectra, and the computed speciation for each DL). Thus, to a 12.5 mM CDCl₃ solution of 1 (1.0 mol equivs, black trace) was added 1.0 mol equiv. of 3. Complex 1.3 partially formed and -as expected- the signal relative to the Hortho proton on 1 was shifted upfield, while those belonging to 3 moved downfield (blue trace). Addition of 1.0 mol equiv of 4 to this mixture partially displaced 3, as evidenced by the upfield shift of the protons on the latter (pink trace). The Hortho signal also moved upfield, indicating increased binding of 1, which was distributed between its free form and the bound ones (1.3 and 1.4). Then, 1.0 mol equivs of 6 were added to the solution, causing a further upfield shift of the signals belonging to 3 and 4, as well as of the Hortho proton (light purple trace). Finally, 1.0 mol equivs of 5 were added to the mixture. This resulted in an upfield shift of the signals belonging to all the previously added ligands and brought the Hortho proton to its saturation value of 7.50 ppm, indicating complete binding.

Thus, at the end of the experiment, the DL contained compounds **1**, **3**, **4**, **6**, and **5** (in order of addition) together with complexes **1•3**, **1•4**, **1•6**, and **1•5** (in order of increased stability). After each addition, the computed amount of free **1** was satisfactorily compared to that estimated from NMR data (see ESI, Figure S53, and Tables S17-S18).

emical Science Accepted Manuscrik

ARTICLE

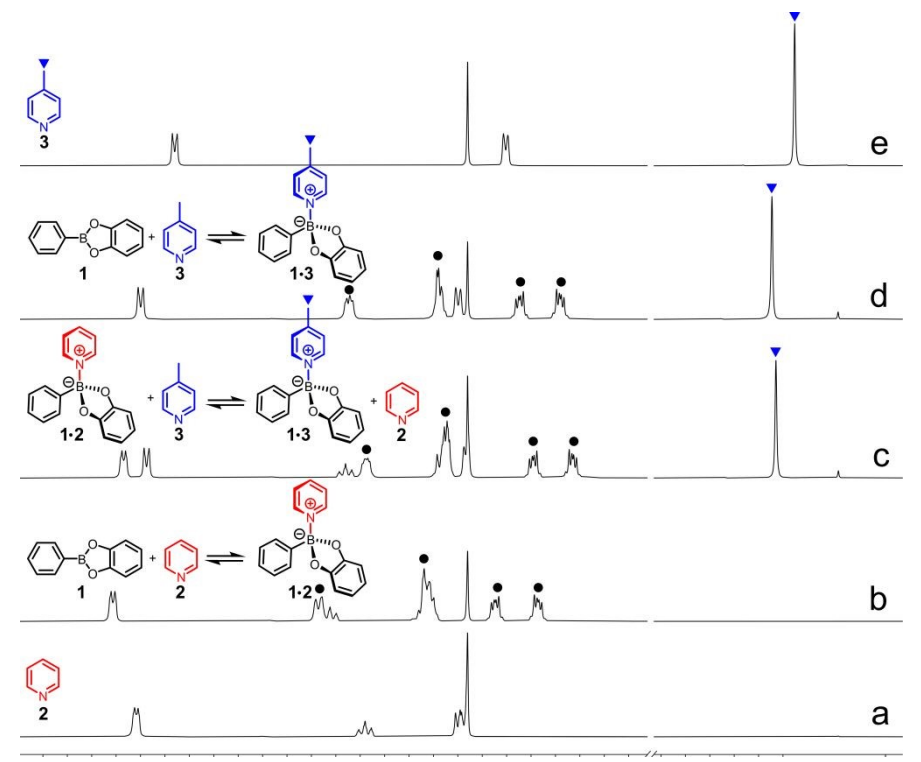


Fig. 4 An exchange experiment in which pyridine 2 (red) and 4-methyl pyridine 3 (blue) compete for phenylboronic acid catechol ester 1 (CDCl₃, 25 °C). All the equilibria are fast on ¹H-NMR time scale with adduct 1•3 prevailing on adduct 1•2 under competitive conditions (trace c). Trace a 12.5 mM 2, trace b 12.5 mM 1 and 2, trace c 12.5 mM 1, 2 and 3, trace d 12.5 mM 3. The black circles are relative to the signals on the 1 backbone.

Next, we investigated the chance to control over time a minimal DL composed of two B–N adducts and related NArHets using an activated carboxylic acid (ACA) as a stimulus. ACAs are used for the operation of dissipative chemical systems, which possess one or more Brønsted basic sites. 77-89 For instance, the DL $1 \cdot 3 + 5 \rightleftharpoons 1 \cdot 5 + 3$ was rapidly obtained by adding in CDCl₃ 15.0 mM equimolar 1, 3 and 5 (Figure 6, 1 H NMR, trace a). As expected from the K_{bind} values reported in Figure 1a, adduct $1 \cdot 5$ largely prevails on $1 \cdot 3$. Addition of 15.0 mM ACA $12 \cdot \text{CO}_2$ H (tribromoacetic acid) causes the extensive protonation of 5, the strongest base present in solution, which is subtracted from the equilibrium. The latter is now shifted to the left with $1 \cdot 3$ prevailing on $1 \cdot 5$.

Comparison between traces a and b of Figure 6 shows that all signals are shifted down-field soon after the addition of 12-CO₂H (trace b). Such shifts are due to protonation of 5 to 5H⁺, whose signals are found down-field shifted with respect to the corresponding ones in adduct 1•5 and to partial association of 3 to 1, which causes the down-field shift of the signals related to both moieties 3 and 1.

However, the new state (Figure 6, trace b) is not an equilibrium one since the ACA conjugate base 12-CO₂- slowly

decarboxylates and the corresponding, just formed carbanion **12**⁻ retakes the proton from **5**H⁺ to give free pyridine **5** and bromoform **12** (traces b to e).

Consequently, the initial equilibrium with $1 \cdot 5$ prevailing on $1 \cdot 3$ is restored (trace e). Thus, when the decarboxylation of ACA 12-CO₂H is complete, the DL goes back to the initial equilibrium state. The above interpretation of the experimental results is strictly consistent with the higher sensitivity of the affinity of the basic nitrogen atoms for the proton than for the boron atom of 1 (for pK_{bind} vs pK_aH^+ p=0.68, see Figure 1d, Figure S33 and the related caption for more details). Furthermore, a computer assisted calculation of the DL speciation based on the pK_aH^+ of 3 and 5 and

ARTICLE

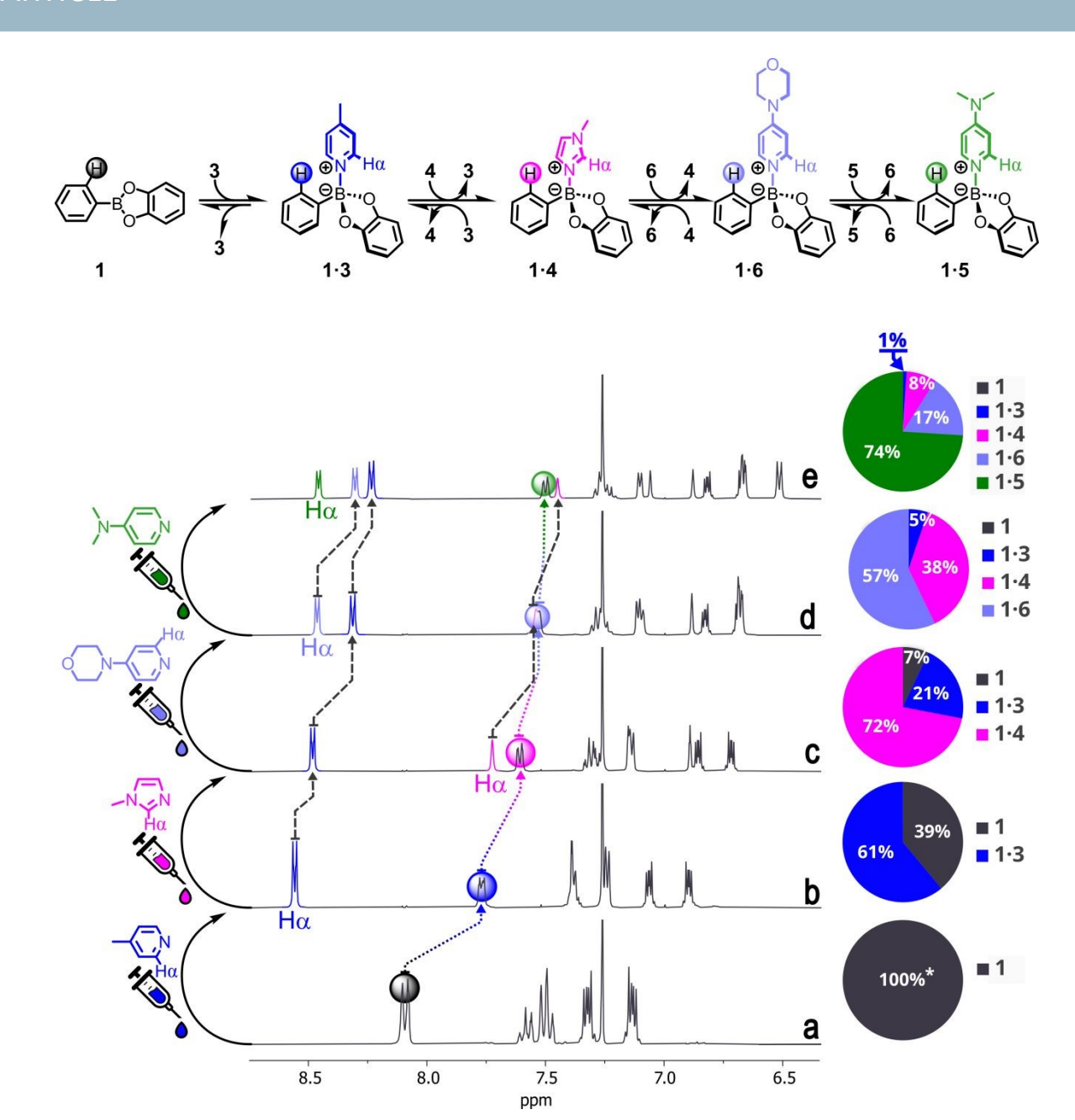


Fig. 5 Top: Simplified reaction scheme for the consecutive generation of DLs containing compounds 1 (black), 3 (blue), 4 (pink), 6 (light purple), and 5 (green, in order of addition) together with complexes 1·3, 1·4, 1·6, and 1·5 (in order of increased stability). Bottom: NMR spectra of 1 (trace a); a mixture of 1 and 3 (trace b); a mixture of 1, 3, and 4 (trace c); a mixture of 1, 3, 4, and 6 (trace d); a mixture of 1, 3, 4, and 5 (trace e). In each spectrum, the signal relative to each Hα proton is highlighted in the same colour as the NArHet (see structures). The H_{ortho} proton is marked with a circle in the colour corresponding to the most prevalent adduct. To the right of each spectrum, a pie chart reports the calculated speciation of each DL. See Tables S17 and S18 for the ChemEQL-assisted speciation of the mixtures. All compounds are added 12.5 mM in CDCl₃, the spectra are recorded at 25 °C. Only the aromatics region is shown. See Figure S53 for the full spectra. * = In the absence of any ligands, 1 is in equilibrium with a small amount (<5% in our conditions) of phenylboronic acid and catechol due to partial hydrolysis from traces of water in the solvent. The addition of NArHets suppresses this side-reaction.

Shemical Science Accepted Manu

ARTICLE

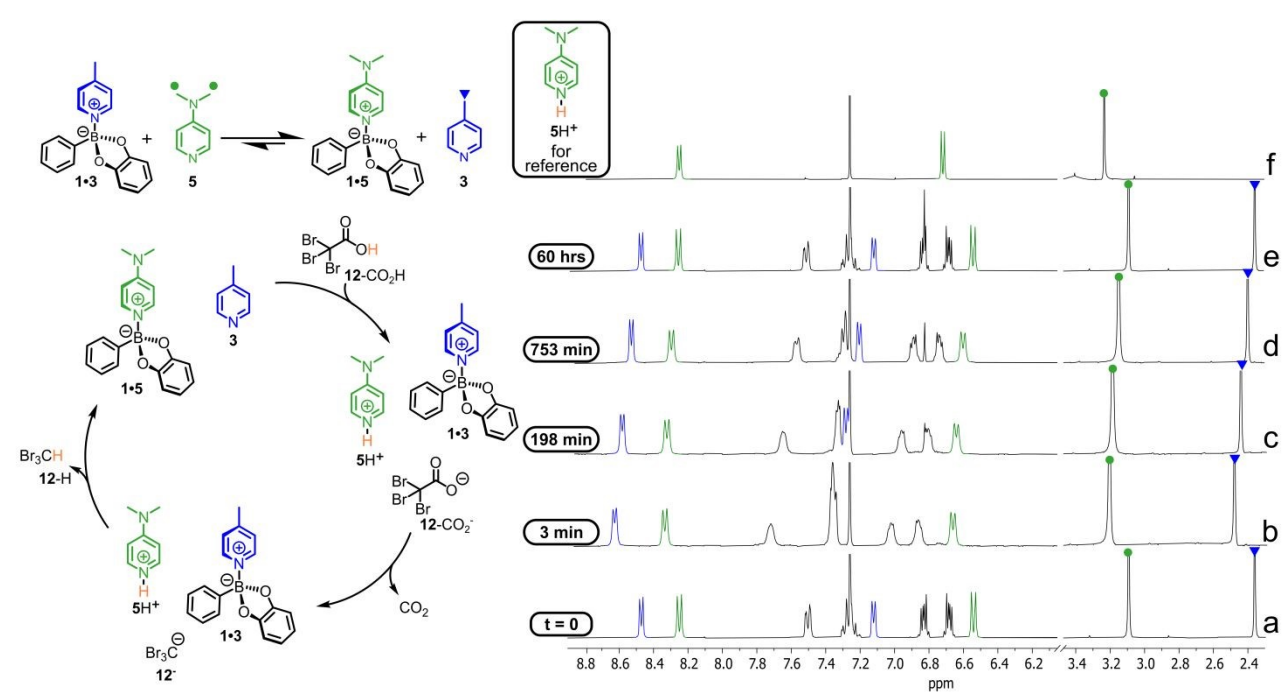


Fig. 6 A minimal DL composed by 1•5, 1•3, and related free building blocks driven by ACA 12-CO₂H (see text). All compounds (1, 3, 5 and 12-CO₂H) are added in solution at 15.0 mM concentration (CDCl₃, 25 °C). On each spectrum, the relevant signals for 3 are marked in blue, while those of 5 are coloured in green.

Compounds 1, 3 and 5, 10.0 mM each, were added in CDCl₃ at 25 °C. The thermodynamic equilibrium with adducts 1.5 prevailing on 1.3, was immediately reached as expected (see state D and trace d in Figure 7 where ¹H NMR spectra of free 1, 1.3 and 1.5 are also reported as traces a, b and c, respectively, for the sake of comparison). Addition of 30.0 mM 12-CO₂H causes protonation of both pyridines 3 and 5, which are liberated in solution affording free 1 (see trace e in Figure 7 recorded at t = 9 min from addition of the ACA). The new state E, which can be defined as a dissipative state, persists as long as the excess acid is present (traces e and f recorded at time t = 9 min and 7 h, are both consistent with the presence of excess acid). When the excess is over (from state F onward), the less basic 3 is firstly deprotonated forming adduct 1.3, as shown by trace g (t = 36 h), which roughly corresponds to state G of Figure 7. At this point the strongest base 5 is still mostly protonated and cannot effectively engage in bonding with 1. Then, ACA 12-CO₂H is further consumed and free base 5 starts to be available for the formation of 1.5 at the expense of 1.3. Eventually, when ACA 12-CO₂H is exhausted, the system goes back to the initial equilibrium state with 1.5 again prevailing on 1.3 (see trace i in Figure 7, t = 5d, which corresponds again to the state D). A corollary of this experiment is that ACA 12-CO₂H can be also used to temporally drive the simple binding equilibrium

between ester **1** and bases **2-6**. And in fact, Figure S40 shows that addition of ACA **12-**CO₂H to complex **1•5**, causes the liberation of **1** in solution due to the transient protonation of **5**. When the decarboxylation of **12-**CO₂H is over, adduct **1•5** is reversibly and completely restored. The process turned out to be fully reversible as demonstrated by an experiment in which three subsequent cycles were triggered by three successive additions of **12-**CO₂H. At the end of each cycle (see Figure S44), adduct **1•5** was found completely reassembled, also proving that bromoform is not detrimental to the B \leftarrow N bond chemistry to any extent. Thus, similarly to what found in the case of the transimination reaction, ^{27,29,89} also in the case of the B \leftarrow N bond exchange, use of ACA allows to drive over time in a predictable fashion dissipative ²⁷ dynamic libraries (DDLs). ²⁸

ARTICLE

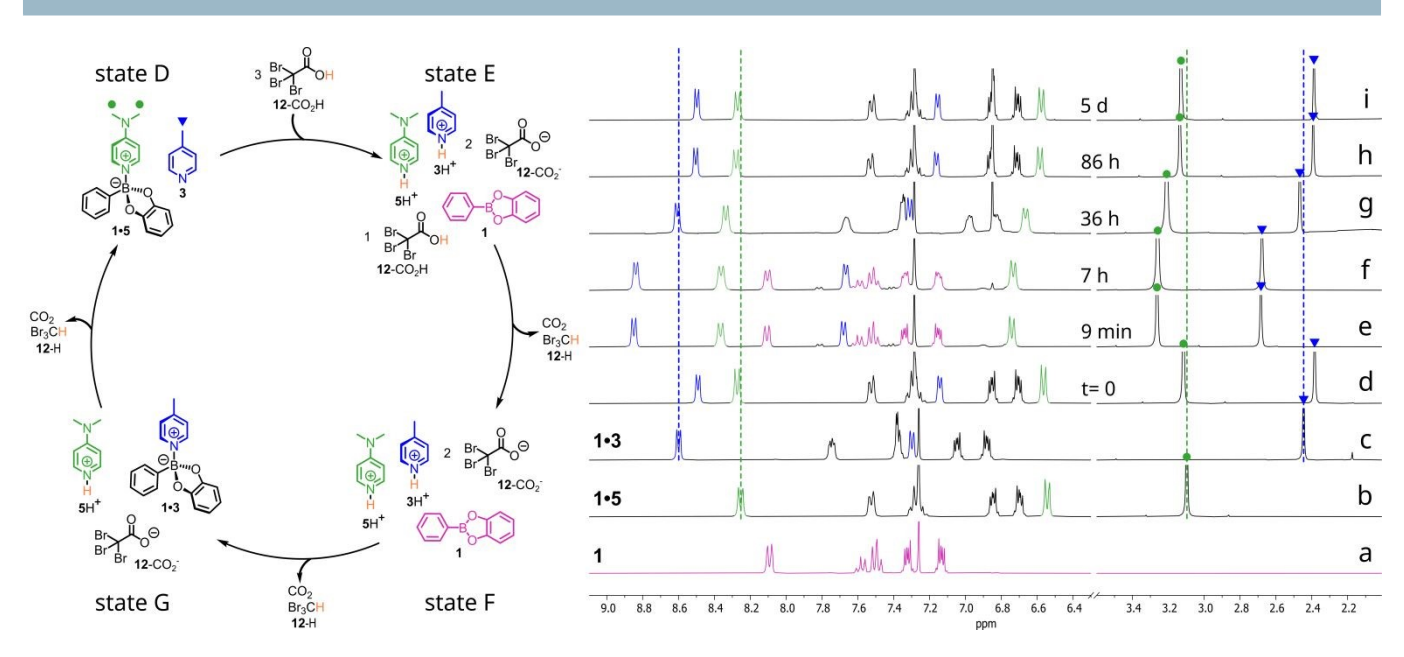


Fig. 7 Behaviour of a DL based on the B←N bond under the action of excess ACA 12-CO₂H. Traces a) 10 mM 1; b) adduct 1•5 obtained by mixing 10 mM 1 with 10 mM 5; c) adduct 1•3 obtained by mixing 10 mM 1 and 10 mM 3; d) equilibrated solution of 10 mM 1, 3 and 5 before addition of 30 mM ACA 12-CO₂H (t = 0); e-i) monitoring over time of solution in trace d after addition of ACA 12-CO₂H. CDCl₃, 25 °C. Dashed vertical lines are guides for the eye. On each spectrum, the relevant signals for 1 are marked in pink, those of 3 in blue, while those of 5 are coloured in green.

Conclusions

In this report we show that the $B \leftarrow N$ bond between phenylboronic acid catechol ester and a series of N-based aromatic heterocycles is fully reversible and can be conveniently used to obtain dynamic libraries of interconverting compounds. In chloroform, such B←N exchange reaction turns out to be rapid on the ¹H NMR time scale and its thermodynamic fate easily predictable from the formation equilibrium constants (K_{bind}) of the exchanging adducts. Moreover, it is shown that the exchange reactions among B←N adducts as well as their formation can be finely controlled over time in a dissipative fashion using activated carboxylic acids (ACAs). It is expected that such reversible interaction will be exploited in the next future for a number of applications such as i) the generation of dynamic libraries composed of more complex chemical structures whose composition can be controlled in a dissipative fashion, ii) the design of boron-based receptors for NArHet anchoring groups with the chance to control the related binding process over the time, iii) the achievement of stimuli responsive materials and dynamic polymer networks based on the exchange of the N-donor species.

Author contributions

Conceptualization: FF, GC, and SDS. Data Curation: FF, GC, MDA, and CM. Formal analysis: GC, FF, and CM. Funding acquisition: SDS and CM. Investigation: all authors. Methodology: FF, GC, OL, and MDA. Supervision: FF, CM, and SDS. Writing: FF, GC, MDA, CM, and SDS.

Conflicts of interest

There are no conflicts to declare.

Data availability

The data supporting this article have been included as part of the electronic supplementary information. †

Acknowledgements

We are grateful for support by Ateneo 2022 Sapienza (RG1221815C85AF91). Furthermore, we thank the European Union-NextGenerationEU under the Italian Ministry of University and Research (MUR), for the PRIN project "Chemically-Driven Autonomous Molecular Machines and Other Dissipative Systems" (N° 2022X779KE). CM acknowledges

This article is licensed under a Creative Commons Attribution 3.0 Unported Licence.

Article. Published on 27 November 2025. Downloaded on 28.11.2025 04:14:48.

Journal Name ARTICLE

the support from the COMP-HUB and COMP-R Initiatives, funded by the 'Departments of Excellence' program of the Italian Ministry for University and Research (MIUR, 2018–2022 and MUR, 2023–2027).

Notes and References

- \ddagger The $logK_{bind}$ values also nicely correlate with Mayr's nucleophilicity parameter; the points related to the $logK_{obs}$ of aliphatic amines behave differently (see Figure S61 and Table S29).
- S. J. Rowan, S. J. Cantrill, G. R. L. Cousins, J. K. M. Sanders and J. F. Stoddart, *Angew. Chem. Int. Ed.*, 2002, 41, 898-952.
- J. Reek and S. Otto, Dynamic Combinatorial Chemistry, Wiley-VCH Verlag GmbH & Co, Weinheim, 2010.
- J. Li, P. Nowak and S. Otto, J. Am. Chem. Soc., 2013, 135, 9222– 9239.
- 4 A. Hermann, Chem. Soc. Rev., 2014, 43, 1899-1933.
- 5 Y. Jin, Q. Wang, P. Taynton and W. Zhang, Acc. Chem. Res., 2014, 47, 1575-1586.
- M. Mondal and A. K. H. Hirsch, Chem. Soc. Rev., 2015, 44, 2455-2488.
- 7 M. He and J.-M. Lehn, J. Am. Chem. Soc., 2019, 141, 18560-18569.
- 8 M. Ciaccia and S. Di Stefano, *Org. Biomol. Chem.*, 2015, **13**, 646–654.
- 9 Peter T. Corbett, S. Otto and J. K. M. Sanders, *Chem. Eur. J.*, 2004, **10**, 3139-3143.
- M. Rauschenberg, S. Bomke, U. Karst and B. J. Ravoo, *Angew. Chem. Int. Ed.*, 2010, 49, 7340-7345.
- 11 P. Nowak, M. Colomb-Delsuc, S. Otto and J. Li, J. Am. Chem. Soc., 2015, 137, 10965-10969.
- 12 A. Canal-Martín and R. Pérez-Fernández, Nat. Commun., 2021, 12, 163.
- 13 B. Brisig, J. K. M. Sanders and S. Otto, Angew. Chem. Int. Ed., 2003, 42,1270-1273.
- 14 J. W. Sadownik and D. Philp, Angew. Chem. Int. Ed., 2008, 47, 9965-9970.
- 15 G. Gasparini, M. Dal Molin and L. J. Prins, *Eur. J. Org. Chem.*, 2010, 2429–2440.
- 16 P.-A. R. Breuil and J. N. H. Reek in *Dynamic Combinatorial Chemistry*, ed J. Reek and S. Otto, Wiley-VCH Verlag GmbH & Co, Weinheim, 2010, 91.
- 17 F. Schaufelberger and O. Ramström, J. Am. Chem. Soc., 2016, 138, 7836–7839.
- 18 M. Tena-Solsona, C. Wanzke, B. Riess, A. R. Bausch and J. Boekhoven, *Nat. Commun.*, 2018, **9**, 2044.
- C. M. E. Kriebisch, A. M. Bergmann and J. Boekhoven, J. Am. Chem. Soc., 2021, 143, 7719–7725.
- 20 P. S. Schwarz, L. Tebcharani, J. E. Heger, P. Müller-Buschbaum and J. Boekhoven, *Chem. Sci.*, 2021, 12, 9969–9976.
- 21 M. A. Wurbser, P. S. Schwarz, J. Heckel, A. M. Bergmann, A. Walther and J. Boekhoven, *ChemSystemsChem*, 2021, **3**, e2100015.
- 22 A. H. J. Engwerda, J. Southworth, M. A. Lebedeva, R. J. H. Scanes, P. Kukura and S. P. Fletcher, *Angew. Chem. Int. Ed.*, 2020, **59**, 20361-20366.
- 23 M. G. Howlett, R. J. H. Scanes, and S. P. Fletcher, JACS Au, 2021, 1, 1355-1361.
- 24 S. Yang, G. Schaeffer, E. Mattia, O. Markovitch, K. Liu, A. S. Hussain, J. Ottelé, A. Sood and S. Otto, *Angew. Chem. Int. Ed.*, 2021, 60, 11344-1349.
- B. Liu, M. A. Beatty, C. G. Pappas, K. Liu, J. Ottelé and S. Otto. Angew. Chem. Int. Ed., 2021, 60, 13569 –13573.
- 26 P. S. Schwarz, M. Tena-Solsona, K. Dai and J. Boekhoven, Chem. Commun., 2022, 58, 1284-1297.

- D. Del Giudice, M. Valentini, G. Melchiorre, E. Spatola and S. Di Stefano, Chem. Eur. J., 2022, 28, e20320068539/D5SC07665J
- 28 D. Del Giudice, E. Spatola, M. Valentini, G. Ercolani and S. Di Stefano, ChemSystemsChem, 2022, 4, e202200023.
- 29 M. Valentini, G. Ercolani and S. Di Stefano, Chem. Eur. J., 2024, 30, e202401104.
- J. M. A. Carnall, C. A. Waudby, A. Belenguer, M. C. A. Stuart, J. J.-P. Peyralans and S. Otto, *Science*, 2010, 327, 1502-1502.
- 31 J. Li, P. Nowak and S. Otto, *J. Am. Chem. Soc.*, 2013, **135**, 9222–9239.
- 32 G. Ashkenasy, T. M. Hermans, S. Otto and A. F. Taylor, *Chem. Soc. Rev.*, 2017, **46**, 2543-2554.
- 33 A. G. Orrillo, A. La-Venia, A. M. Escalante and R. L. E Furlan, Chem. Eur. J., 2018, 24, 3141-3146.
- 34 D. Larsen and S. R. Beeren, Chem. Sci., 2019, 10, 9981–9987.
- 35 D. Carbajo, Y. Pérez, J. Bujons and I. Alfonso, *Angew. Chem. Int. Ed.*, 2020, *59*, 17202-17206.
- 36 S. Otto, Acc. Chem. Res., 2022, 55, 145-155.
- 37 P. M. Mitrasinovic, Curr. Org. Synth., 2012, 9, 233-246.
- 38 Z.-H. Zhao, C.-H. Li and J.-L. Zuo, SmartMat, 2023, 4, e1187.
- 39 C. He, J. Dong, C. Xu and X. Pan, ACS Polym. Au, 2023, 3, 5–27.
- 40 B. Chen and F. Jäkle, *Angew. Chem. Int. Ed Engl.*, 2024, **63**, e202313379.
- 41 N. Farfán, H. Höpfl, V. Barba, M. Eugenia Ochoa, R. Santillan, E. Gómez and A. Gutiérrez, *J. Organomet. Chem.*, 1999, **581**, 70–81.
- 42 N. Christinat, R. Scopelliti and K. Severin, *Chem. Commun.*, 2004, **10**, 1158-1159.
- 43 N. Christinat, R. Scopelliti and K. Severin, *J. Org. Chem.*, 2007, **72**, 2192–2200.
- 44 D. Salazar-Mendoza, J. Cruz-Huerta, H. Höpfl, I. F. Hernández-Ahuactzi and M. Sanchez *Cryst. Growth Des.*, 2013, **13**, 2441–2454.
- 45 C. J. Hartwick, S. P. Yelgaonkar, E. W. Reinheimer, G. Campillo-Alvarado and L. R. MacGillivray, *Cryst. Growth Des.*, 2021, 21, 4482–4487.
- 46 B. Icli, E. Sheepwash, T. Riis-Johannessen, K. Schenk, Y. Filinchuk, R. Scopelliti and K. Severin, *Chem. Sci.*, 2011, 2, 1719-1721.
- 47 A. Dhara and F. Beuerle, *Chem. Eur. J.*, 2015, **21**, 17391 17396.
- 48 N. Christinat, R. Scopelliti and K. Severin, *Chem. Commun.*, 2008, **31**, 3660–3662.
- 49 X. Xiao, D. Xiao, G. Sheng, T. Shan, J. Wang, X. Miao, Y. Liu, G. Li, Y. Zhu, J. L. Sessler and F. Huang, *Sci. Adv.*, 2023, 9, eadi1169.
- 50 G. Campillo-Alvarado, E. C. Vargas-Olvera, H. Höpfl, A. D. Herrera-España, O. Sánchez-Guadarrama, H. Morales-Rojas, L. R. MacGillivray, B. Rodríguez-Molina and N. Farfán, *Cryst. Growth Des.*, 2018, 18, 2726–2743.
- 51 G. Campillo-Alvarado, K. P. D'mello, D. C. Swenson, S. V. Santhana Mariappan, H. Höpfl, H. Morales-Rojas and L. R. MacGillivray, *Angew. Chem. Int. Ed Engl.*, 2019, **58**, 5413–5416.
- 52 G. Campillo-Alvarado, C. Li, Z. Feng, K. M. Hutchins, D. C. Swenson, H. Höpfl, H. Morales-Rojas and L. R. MacGillivray, Organometallics, 2020, 39, 2197–2201.
- 53 A. D. Herrera-España, H. Höpfl and H. Morales-Rojas, *ChemPlusChem*, 2020, **85**, 548–560.
- 54 K. K. Ray, G. Campillo-Alvarado, H. Morales-Rojas, H. Höpfl, L. R. MacGillivray and A. V. Tivanski, *Cryst. Growth Des.*, 2020, 20, 3–8.
- 55 J. D. Loya, S. A. Agarwal, N. Lutz, E. W. Reinheimer and G. Campillo-Alvarado, *CrystEngComm*, 2024, **26**, 4017–4021.
- 56 E. Sheepwash, V. Krampl, R. Scopelliti, O. Sereda, A. Neels and K. Severin, *Angew. Chem. Int. Ed.*, 2011, **50**, 3034–3037.

Shemical Science Accepted Manuscript

ARTICLE Journal Name

- 57 J. Cruz-Huerta, D. Salazar-Mendoza, J. Hernández-Paredes, I. F. Hernández Ahuactzi and H. Höpfl, Chem. Commun., 2012, 48, 4241-4243.
- 58 A. J. Stephens, R. Scopelliti, F. F. Tirani, E. Solari and K. Severin, ACS Mater. Lett., 2019, 1, 3-7.
- 59 F. Li, X. Xiao and Q. Xu, Chem, 2023, **9**, 13–15.
- 60 H. Zhang, Y. Li, L. Chen, Y. Yang, H. Lin, S. Xiang, B. Chen and Z. Zhang, Chem, 2023, 9, 242-252.
- 61 C.-H. Liu, L. Chen, H. Zhang, Y. Li, H. Lin, L. Li, J. Wu, C. Liu, Z.-M. Ye, S. Xiang, B. Chen and Z. Zhang, Chem, 2023, 9, 3532-
- 62 N. Christinat, E. Croisier, R. Scopelliti, M. Cascella, U. Röthlisberger and K. Severin, Eur. J. Inorg. Chem., 2007, 5177-
- E. Sheepwash, N. Luisier, M. R. Krause, S. Noé, S. Kubik and K. Severin, Chem. Commun., 2012, 48, 7808-7810.
- 64 N. Luisier, R. Scopelliti and K. Severin, Soft Matter, 2016, 12, 588-593.
- J. Cruz-Huerta, G. Campillo-Alvarado, H. Höpfl, P. Rodríguez-Cuamatzi, V. Reyes-Márquez, J. Guerrero-Álvarez, D. Salazar-Mendoza and N. Farfán-García, Eur. J. Inorg. Chem., 2016, 355-365.
- 66 F. Vidal, J. Gomezcoello, R. A. Lalancette and F. Jäkle, J. Am. Chem. Soc., 2019, 141, 15963-15971.
- X. Wang, L. Zhang, X. Wang, T. Cheng, M. Xue, Q. Dong, Y. Peng and Q. Zhang, Adv. Funct. Mater., 2024, 202401362.
- 68 X. Sun, B. M. Chapin, P. Metola, B. Collins, B. Wang, T. D. James and E. V. Anslyn, Nat. Chem., 2019, 11, 768-778.
- C. R. Groom, I. J. Bruno, M. P. Lightfoot and S. C. Ward, ActaCryst.B, 2016, 72, 171-179.
- 70 W. Clegg, A. J. Scott, F. E. S. Souza and T. B. Marder, Acta Crystallogr., Sect. C: Cryst. Struct. Commun., 1999, 55, 1885-
- 71 F. Neese, Wiley Interdiscip. Rev. Comput. Mol. Sci., 2012, 2, 73-78.
- 72 Neese, F. Wiley Interdiscip. Rev.: Comput. Mol. Sci., 2025, 15, e70019.
- 73 S. Grimme, A. Hansen, S. Ehlert and J.-M. Mewes, J. Chem. Phys., 2021, 154, 064103.
- 74 A. V. Marenich, C. J. Cramer and D. G. Truhlar, J. Phys. Chem. *B*, 2009, **113**, 6378–6396.
- 75 P. Erdmann, L. M. Sigmund, M. Schmitt, T. Hähnel, L. B. Dittmer and L. Greb, *Chemphyschem*, 2024, **25**, e202400761.
- 76 R. Lo, D. Manna, M. Lamanec, M. Dračínský, P. Bouř, T. Wu, G. Bastien, J. Kaleta, V. M. Miriyala, V. Špirko, A. Mašínová, D. Nachtigallová and P. Hobza, Nat. Commun., 2022, 13, 2107.
- J. A. Berrocal, C. Biagini, L. Mandolini and S. Di Stefano, Angew. Chem. Int. Ed., 2016, 55, 6997-7001.
- 78 C. Biagini, F. Di Pietri, L. Mandolini, O. Lanzalunga and S. Di Stefano, Chem. Eur. J., 2018, 24, 10122–10127.
- C. Biagini, G. Capocasa, V. Cataldi, D. Del Giudice, L. Mandolini and S. Di Stefano, Chem. Eur. J., 2019, 25, 15205-15211.
- C. Biagini and S. Di Stefano, Angew. Chem. Int. Ed., 2020, 59, 8344-8354.
- 81 D. Del Giudice, F. Tavani, M. Di Berto Mancini, F. Frateloreto, M. Busato, D. Oliveira De Souza, F. Cenesi, O. Lanzalunga, S. Di Stefano and P. D'Angelo, Chem. Eur. J., 2022, 28, e202103825.
- 82 F. Frateloreto, F. Tavani, M. Di Berto Mancini, D. Del Giudice, G. Capocasa, I. Kieffer, O. Lanzalunga, S. Di Stefano and P. D'Angelo, J. Phys. Chem. Lett., 2022, 13, 5522-5529
- 83 D. Del Giudice, F. Frateloreto, C. Sappino and S. Di Stefano, Eur. J. Org. Chem., 2022, e202200407.
- 84 M. Valentini, F. Frateloreto, M. Conti, R. Cacciapaglia, D. Del Giudice and S. Di Stefano, Chem. Eur. J., 2023, 29, e202301835.
- 85 D. Del Giudice and S. Di Stefano, Acc. Chem. Res., 2023, 56, 889-899.

- 86 G. Capocasa, F. Frateloreto, S. Correale Cavallari, M. Valentini O. Lanzalunga and S. Di Stefano, Chem. Euro36/D20247630 e202303897.
- 87 F. Frateloreto, G. Capocasa, A. D'Arrigo, M. De Angelis, O. Lanzalunga, S. Di Stefano, ChemSystemsChem. 2025, 7, e202500008
- 88 M. De Angelis, G. Capocasa, F. Ranieri, G. Mazzoccanti, F. Frateloreto, S. Manetto, A. Fagnano, C. Massera, G. Olivo, F. Ceccacci, A. Ciogli, S. Di Stefano, Angew. Chem. Int. Ed. 2025, e202513917.
- 89 G. Melchiorre, L. Visieri, M. Valentini, R. Cacciapaglia, A. Casnati, L. Baldini, J. A. Berrocal and S. Di Stefano, J. Am. Chem. Soc., 2025, 147, 11327-11335.

Open Access Article. Published on 27 November 2025. Downloaded on 28.11.2025 04:14:48. This article is licensed under a Creative Commons Attribution 3.0 Unported Licence.

Data availability

The data supporting this article have been included as part of the electronic supplementary information. †